

SIMULTANEOUS ATTITUDE CONTROL AND MODES ESTIMATION FOR FLEXIBLE SPACECRAFT USING ADAPTIVE CONTROL AND INTEGRAL CONCURRENT LEARNING

**R. Bevilacqua^{*}, C. Riaño-Rios[†],
A. Sinclair[‡]**

In this paper we lay the foundations for attitude control and simultaneous mode estimation of highly flexible spacecraft. Adaptive control (AC) combined with integral concurrent learning (ICL) enable quantifiable finite time excitation of the system while it is being controlled, thus providing convergence of unknown or uncertain parameters to their true values. Rigorous Lyapunov proofs are provided, guaranteeing stability of the controlled system and convergence of the unknown parameters. The focus is controlling the spacecraft attitude and using the behavior of key locations of most flexible components (i.e., the extremities), setting the natural frequencies and damping ratios as the uncertain parameters to estimate. The preliminary results here presented are encouraging and we envision this technique to be transformative in the way we control flexible space structures with uncertain structural characteristics. This work is motivated by the Air Force Space Solar Power Incremental Demonstrations and Research (SSPIDR) project, and more generally, future spacecraft with deployable and large flexible appendages.

INTRODUCTION

Standard techniques to operate flexible spacecraft separate control and estimation, as presented, for example, by the Air Force Research Laboratory (AFRL) in reference 1. Several researchers approach the control problem by assuming a good knowledge of the modes of vibration for the system, compensating for uncertainties using feedback controllers whose performances are affected by the level of uncertainty (see, for example reference 2). Others focus only on on-orbit modes estimation, as seen in references 3 and 4; note that these references are decades apart.

This paper investigates the possibility to perform attitude control for a flexible spacecraft and simultaneously estimate, via finite time quantifiable excitation, the main parameters related to its flexible dynamics. The authors have recently demonstrated the preliminary potential of adaptive control combined with integral concurrent learning for underactuated spacecraft exploiting only natural forces and torques to control within a formation (5-7).

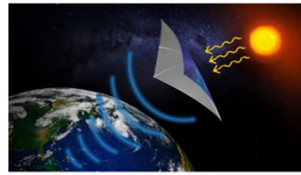
The motivation for this paper originates from a renewed interest in space structures and

^{*} Professor, Advanced Autonomous Multiple Spacecraft (ADAMUS) laboratory, Aerospace Engineering, Embry-Riddle Aeronautical University, 1 Aerospace Blvd., LB-262, FL 32114.

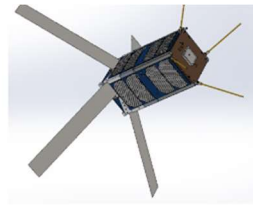
[†] AOCS Guidance, Navigation and Control Engineer, Satellogic, Scalabrin Ortiz 3333 3rd Floor, Buenos Aires, Argentina.

[‡] Senior Aerospace Engineer, Air Force Research Laboratory, Space Vehicles Directorate, 3550 Aberdeen Ave SE, Kirtland AFB, NM 87117

particularly spacecraft equipped with deployables, whose flexible dynamics will present a wide range of frequencies and amplitudes of deformation (Figure 1).



AFRL's Space Solar Power Incremental and Demonstrations Research Project (SSPIDR)



D3 CubeSat designed by the ADAMUS laboratory

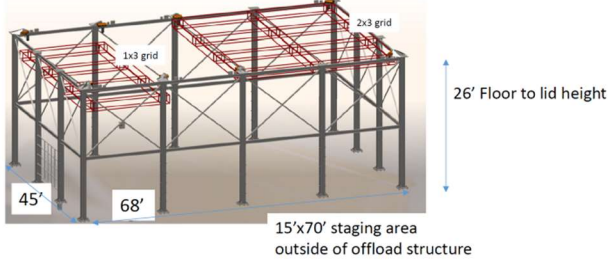


Figure 1 Examples of future and current spacecraft missions involving flexible deployables (top, left and right respectively) and recent Air Force facilities committed to the characterization of elastic space systems (bottom).

To support the previous statement, we note that the AFRL Space Vehicle Directorate recently opened the new Deployable Structures Laboratory, or DeSeL (reference 8 and Figure 1). DeSeL represents the state-of-the-art technology for on-the-ground experimentation of deployable systems. An active Gravity Off-Load Follower (GOLF) cart system is being currently developed, intended to have three degrees of freedom (attitude motion) which could foreseeably provide the capability for large low-frequency motions.

Past examples of deployable spacecraft include the Deployable Optical Telescope (DOT, 9-10); more than a decade ago a substantial effort was undertaken to ground-test part of the system, but only for high frequencies, low amplitude deformations. The Mid-Deck Active Control Experiment (MACE, 11) is an AFRL example of flexible system control using a small-scale experiment on the Space Shuttle. Today's counterpart for this approach is the CubeSat format (12).

Large space structures and those with high dimensional ratio between deployed and stowed configurations are extremely difficult to test on the ground; the above mentioned SSPIDR and Drag Deorbit Device (D3; reference 13) missions fall under this category, and their operations would benefit from a real-time on-board estimation of the flexible behavior.

This paper aims at creating the foundations for attitude/orbit maneuvering/excitation and simultaneous mode estimation of highly flexible spacecraft, enabling on-orbit autonomous testing of the entire structure, thus saving cost and time on the ground, and capturing unknown deviations from computer models that may be caused by poor modeling, storage, and launch stresses.

The paper is organized as follows: we first present a commonly used dynamics model for

spacecraft equipped with flexible appendages, then proceed to introducing a simplified study case, where actual displacements are used in the dynamics, instead of modal coordinates. After the dynamics sections the paper proceeds to illustrate the proposed adaptive control law with integral concurrent learning, along with Lyapunov stability proof. A sample numerical simulation is presented before drawing conclusions and discussing future work.

COMMONLY USED MODEL FOR FLEXIBLE SPACECRAFT

The attitude dynamics of spacecraft with flexible components are often modeled as a rigid body connected through springs and dampers to point masses distributed throughout the flexible appendage(s), which are also connected to each other according to the spacecraft geometry. A commonly used simplified model is expressed in terms of the modal coordinates, which are a linear combination of the point mass(es) displacement(s) and decouple the dynamics of flexible appendages. The dynamics have the form:

$$\begin{aligned} J\dot{\omega} + \delta^T \ddot{\eta} &= -\omega \times (J\omega + \delta^T \eta) + u \\ \ddot{\eta} + C\dot{\eta} + K\eta &= -\delta\dot{\omega} \end{aligned}$$

J : Total inertia matrix
 ω : inertial angular velocity
 η : vector of modal coordinates
 δ : coupling matrix
 u : external torques
 C : damping matrix
 K : stiffness matrix

Natural frequencies and damping coefficients associated with flexible modes are contained in matrices C and K

Equation 1

Modal coordinates and matrices C and K can be approximately obtained using different methods. However, they are subject to uncertainty due to modeling simplifications and structural changes during storage, launch and/or deployment, among others. If such uncertainties are considered to design an attitude controller, the use of actual displacements instead of modal coordinates is desired, since they can be directly measured by placing sensors on the structure. This work proposes the use a dynamic model in terms of the displacements to design an adaptive controller that incorporates Integral Concurrent Learning into the adaptation law to provide online estimation of uncertain parameters while controlling the spacecraft attitude.

A SIMPLIFIED DEFORMATION-BASED MODEL FOR FLEXIBLE SPACECRAFT

Consider a simplified example of a spacecraft with its main rigid body connected to a flexible appendage including a mass, spring, and damper, as shown in Figure 2. The model for this spacecraft has the form:

$$\begin{aligned} J\dot{\omega} + j\omega + \delta^T \ddot{x} + \omega \times (J\omega + \delta^T \dot{x}) &= u \\ m\ddot{x} + C\dot{x} + Kx - 2m\omega_z^2 - 2ml\omega_x\omega_y - 2\omega_x^2 &= -\delta\dot{\omega} \end{aligned}$$

Equation 2

where m is the point mass representing the inertia of the flexible appendage, x its displacement due to flexibility, and l the distance between the spacecraft main body and the axis of displacement. Additionally, $\delta = [0 \ 0 \ -lm]$, $J = J_s + J_m$, where J_s is the inertia matrix of main hub, and J_m the contribution of m to the inertia matrix. Note that C and K are not diagonal matrices (in the single mass-spring-damper case they are scalars).

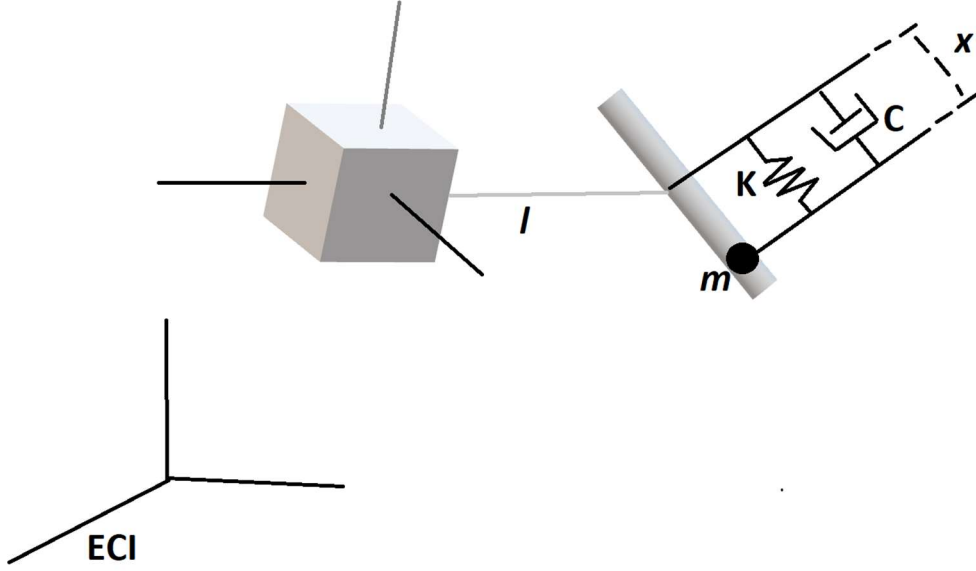


Figure 2 single mass-spring-damper model for a spacecraft with a flexible appendage.

Neglecting second order coupling terms we get:

$$\begin{aligned} J^* \dot{\omega} + J^* \omega + \delta^T \ddot{x} + \omega \times (J^* \omega + \delta^T \dot{x}) &= u \\ m \ddot{x} + C \dot{x} + Kx &= -\delta \dot{\omega} \end{aligned}$$

Consider C and K being uncertain. Moreover, the exact location of the point mass (l), as well as the mass (m) are not accurately known. Note that J_m^* and δ depend on m and l , then J^* and J^* are also uncertain. If the orientation of the spacecraft is represented with the quaternion q , then the attitude mismatch with respect to a desired orientation q_d can be expressed as the error quaternion e , which obeys the following kinematics for its vector and scalar parts

$$\begin{aligned} \dot{e}_v &= \frac{1}{2} (e_v^x + e_0 I_3) \tilde{\omega}, \\ \dot{e}_o &= -\frac{1}{2} e_v^T \tilde{\omega}, \end{aligned}$$

Equation 3

where $\tilde{\omega} = \omega - \tilde{R} \omega_d$, ω_d is the desired angular velocity and \tilde{R} is the rotation matrix from the desired to the actual body frame.

The simplified model presented in this section could be expanded to multiple mass-spring-damper systems, installed at different locations and different orientations with respect to the main hub. Despite being beyond the scope of this paper, this approach would enable deformation-based modeling of the system, where the lump parameter subsystems are not fully known but can be estimated online, as described in the remainder of the paper.

CONTROL APPROACH

The control objective is to correct for quaternion errors, that is: $\tilde{R} \rightarrow I_3$, in the presence of uncertainty in m , l , C and K . Additionally, we intend to identify the uncertainties online. Let us define the auxiliary state $\mathbf{r} = \tilde{\boldsymbol{\omega}} + \alpha \mathbf{e}_v$, where α is a positive definite, constant control gain matrix. Driving $\mathbf{r} \rightarrow 0$ is sufficient to drive $\tilde{R} \rightarrow I_3$. Taking the time derivative of \mathbf{r} , pre-multiplying by J_s , and substituting the dynamics, we obtain the open-loop error system:

$$J_s \dot{\mathbf{r}} = -\boldsymbol{\omega} \times (J_s \boldsymbol{\omega} + J_m^* \boldsymbol{\omega} + \delta^T \dot{\mathbf{x}}) - J_m^* \boldsymbol{\omega} + \delta^T \left(\frac{K}{m} \mathbf{x} + \frac{C}{m} \dot{\mathbf{x}} \right) - J_s (\dot{\tilde{R}} \boldsymbol{\omega}_d + \tilde{R} \dot{\boldsymbol{\omega}}_d) + J_s \alpha \dot{\mathbf{e}}_v + \mathbf{u}$$

Equation 4

Where the terms in red are uncertain. We then define the following linear parameterization

$$Y(\mathbf{x}, \dot{\mathbf{x}}, \boldsymbol{\omega}) \Theta = -\boldsymbol{\omega} \times (J_m^* \boldsymbol{\omega} + \delta^T \dot{\mathbf{x}}) - J_m^* \boldsymbol{\omega} + \delta^T \left(\frac{K}{m} \mathbf{x} + \frac{C}{m} \dot{\mathbf{x}} \right)$$

and

$$\Theta = [J_{mxz}, J_{mxy}, J_{mxz}, J_{myy}, J_{myz}, J_{mzz}, \dot{J}_{mxz}, \dot{J}_{mxy}, \dot{J}_{mxz}, \dot{J}_{myy}, \dot{J}_{myz}, \dot{J}_{mzz}, \delta^T, \frac{\delta_1 C}{m}, \frac{\delta_2 C}{m}, \frac{\delta_3 C}{m}, \frac{\delta_1 K}{m}, \frac{\delta_2 K}{m}, \frac{\delta_3 K}{m}]^T \in \mathbb{R}^{21}$$

Assumption 1: the vector Θ is constant, e.g., it contains the mean of the inertia components.

We propose the following control law:

$$\mathbf{u} = \boldsymbol{\omega} \times J_s \boldsymbol{\omega} + J_s (\tilde{R} \boldsymbol{\omega}_d + \tilde{R} \dot{\boldsymbol{\omega}}_d) - J_s \alpha \dot{\mathbf{e}}_v - Y \hat{\Theta} - \beta \mathbf{e}_v - K_1 \mathbf{r}$$

where K_1 is a positive definite, constant control gain matrix, β is a positive, constant control gain, and $\hat{\Theta}$ is the estimate of Θ . To design $\hat{\Theta}$, we define the following integrals over a time window of size Δt

$$\begin{aligned} \mathcal{Y}(\Delta t, t) &= \int_{t-\Delta t}^t Y(\sigma) d\sigma \\ \mathcal{U}(\Delta t, t) &= \int_{t-\Delta t}^t [\mathbf{u}(\sigma) - \boldsymbol{\omega}(\sigma) \times J_s \boldsymbol{\omega}(\sigma) - J_s (\dot{\tilde{R}}(\sigma) \boldsymbol{\omega}_d(\sigma) + \tilde{R}(\sigma) \dot{\boldsymbol{\omega}}_d(\sigma) - \alpha \dot{\mathbf{e}}_v(\sigma))] d\sigma \end{aligned}$$

Equation 8

and the ICL-based, adaptation law is designed as

$$\dot{\hat{\Theta}} = \text{proj}(\Gamma \mathcal{Y}^T \mathbf{r} + \Gamma K_{ICL} \sum_{i=1}^N \mathbf{y}_i^T (J_s(\mathbf{r}(t) - \mathbf{r}(t - \Delta t)) - \mathbf{u}_i - \mathbf{y}_i \hat{\Theta}))$$

where $\mathbf{y}_i = \mathcal{Y}(t_i)$, $\mathbf{u}_i = \mathcal{U}_i(t_i)$, and Γ , K_{ICL} are positive definite, constant adaptation gains matrices. The verifiable ICL finite excitation condition considers that there exists a time T , such that

$$\lambda_{min}\{\sum_i^N \mathbf{y}_i^T \mathbf{y}_i\} \geq \bar{\lambda} \quad \text{for } t \geq T$$

where $\lambda_{min}\{\cdot\}$ is the minimum eigenvalue of $\{\cdot\}$, and $\bar{\lambda}$ is a positive, user defined constant.

Considering the following candidate Lyapunov function

$$V(t) = \frac{1}{2} \mathbf{r}^T J_s \mathbf{r} + \beta \mathbf{e}_v^T \mathbf{e}_v + (1 - \mathbf{e}_0)^2 + \frac{1}{2} \tilde{\Theta} \Gamma^{-1} \tilde{\Theta}$$

Equation 11

and under the assumption that J_m^*, \dot{J}_m^* are physical quantities bounded by known constants, then, for $t < T$, the following globally uniformly ultimately bounded result can be obtained:

$$\|y\| \leq \epsilon_1 \exp(-\epsilon_2 t) + \epsilon_3 \quad \text{Equation 12}$$

where $y = [r^T \ e_v^T]^T$, and ϵ_1, ϵ_2 , and ϵ_3 are known, positive constants.

For $t \geq T$, the following globally uniformly ultimately bounded result, including the uncertain parameters, can be obtained:

$$\|z\| \leq \epsilon_4 \exp(-\epsilon_5 t) + \epsilon_6 \quad \text{Equation 13}$$

where $z = [y^T \ \tilde{\Theta}^T]^T$, ϵ_4, ϵ_5 , and ϵ_6 are positive known constants.

Recall that:

$$\begin{aligned} \Theta = & [J_{mxx}, J_{mxy}, J_{mxz}, J_{myy}, J_{myz}, J_{mzz}, \dot{J}_{mxx}, \dot{J}_{mxy}, \dot{J}_{mxz}, \dot{J}_{myy}, \dot{J}_{myz}, \dot{J}_{mzz}, \\ & \delta^T, \frac{\delta_1 C}{m}, \frac{\delta_2 C}{m}, \frac{\delta_3 C}{m}, \frac{\delta_1 K}{m}, \frac{\delta_2 K}{m}, \frac{\delta_3 K}{m}]^T \in \mathbb{R}^{21} \end{aligned}$$

And note that, if the knowledge of Θ is improved from an inaccurate initial guess, the natural frequency ω_n and damping coefficient ζ can be recovered since

$$\omega_n = \sqrt{\frac{K}{m}} \quad , \quad \zeta = \frac{C}{2m\omega_n}$$

NUMERICAL SIMULATION

In this section, the proposed controller is tested without (Sim 1) and with (Sim 2) the ICL in the adaptation law. The spacecraft is initially tumbling at angular rates of up to 5 RPM and the desired orientation is alignment with the inertial frame.

To facilitate the tuning process, the size of Θ has been reduced by making the following assumptions:

Assumption 2: The time derivative of J_m is negligible.

Assumption 3: Only non-zero elements of J_m are those of its diagonal.

Assumption 4: δ_1 and δ_2 are known zero.

The vector of uncertain parameters is then defined as $\Theta = [J_{mxx}, J_{myy}, J_{mzz}, \delta_3, \frac{\delta_3 C}{m}, \frac{\delta_3 K}{m}]^T \in \mathbb{R}^6$.

The simulation parameters are:

$$\zeta = 0.05 \quad \omega_n = 1.0973 \frac{rad}{s} \quad m = 0.5 \text{ kg} \quad M = 200 \text{ kg} \quad K = \omega_n^2 \quad C = 2\zeta\omega_n \quad l = 0.6 \text{ m}$$

$$H = 0.5 \text{ m} \quad W = 0.5 \text{ m} \quad L = 1 \text{ m}$$

$$J_s = \begin{bmatrix} \frac{1}{12}M(H^2 + W^2) & 0 & 0 \\ 0 & \frac{1}{12}M(L^2 + W^2) & 0 \\ 0 & 0 & \frac{1}{12}M(L^2 + H^2) \end{bmatrix}$$

$$\boldsymbol{\omega}_0 = [0.1, -0.5, -0.5]^T \frac{rad}{s} \quad \boldsymbol{q}_0 = [0.8924, -0.99, 0.2391, 0.3696]^T \quad x_0 = 1 \times 10^{-3} m$$

$$\widehat{\boldsymbol{\Theta}}_0 = [0, 0.22, 0.12, -0.2, -0.04, -0.6]^T$$

$$\bar{\lambda} = 4.2 \times 10^{-18} \text{ (Sim 2 only)}$$

$$\Gamma = 3 \text{ diag}([1, 1, 1, 30, 2, 10]) \text{ (Sim 1)}, \Gamma = 0.8 \text{ diag}([1, 1, 1, 30, 2, 10]) \text{ (Sim2)}$$

$$K_{ICL} = 500 \text{ diag}([0.01, 0.01, 0.01, 0.8, 10, 1]) \text{ (Sim2 only)}$$

$$K_1 = 0.005 I_3 \text{ (Sim 1)}, K_1 = 0.01 I_3 \text{ (Sim 2)}$$

$$\alpha = 0.38 I_3 \text{ (Sim 1)}, \alpha = 0.1 I_3 \text{ (Sim 2)} \quad \beta = 0.005$$

The following plots show results of Sim 1 (with the ICL term of the adaptation law turned off) in terms of orientation (\boldsymbol{q}), angular velocity ($\boldsymbol{\omega}$), point mass displacement (x), torques (\boldsymbol{u}) and estimation of the unknown vector.

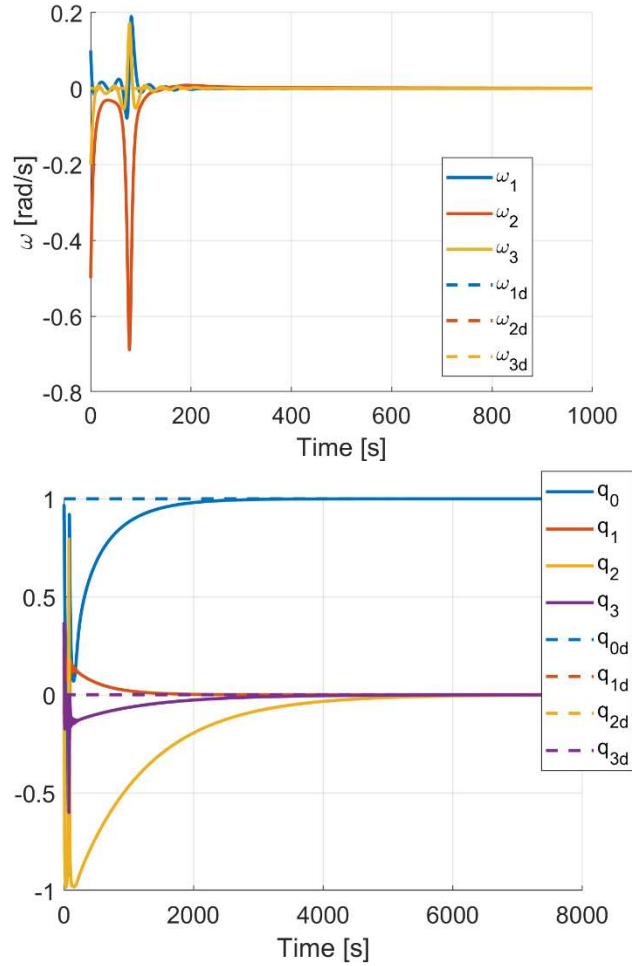


Figure 3 Sim 1 (ICL off) numerical results: spacecraft angular velocity vs desired angular velocity (top), spacecraft quaternion vs desired quaternion (bottom).

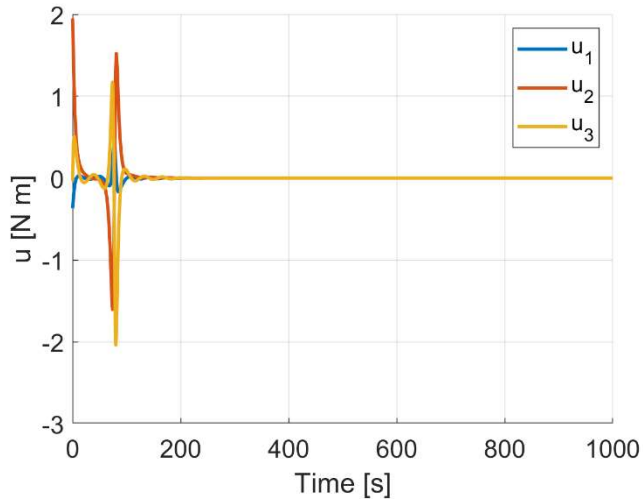


Figure 4 Sim 1 (ICL off) numerical results: spacecraft control torques.

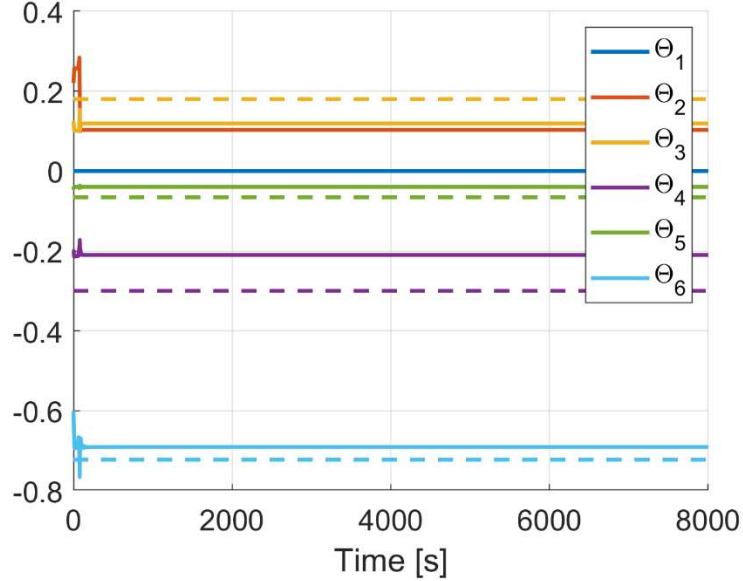


Figure 5 Sim 1 (ICL off) numerical results: vector of estimated unknowns vs true values.

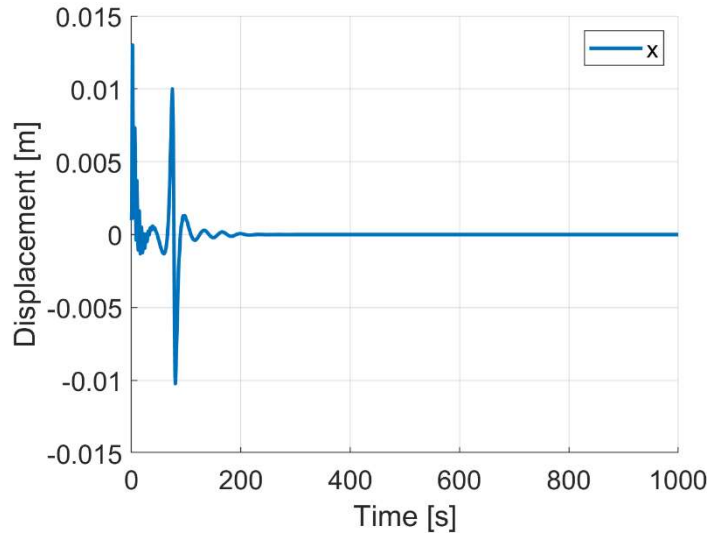


Figure 6 Sim 1 (ICL off) numerical results: lumped mass displacement.

The results from this simulation have shown that the adaptive controller can stabilize the spacecraft while compensating for the uncertain parameters, however, the final values of the estimated parameters (solid lines) have clearly converged to values far apart from their real values (dashed lines). This controller has been tuned so that the applied control effort is similar in magnitude to that of Sim 2, which includes ICL.

The following plots show results of Sim 2 (with the ICL term of the adaptation law turned on) in terms of orientation (\mathbf{q}), angular velocity ($\boldsymbol{\omega}$), point mass displacement (x), torques (\mathbf{u}), estimation of the unknown vector, and finite excitation condition ($\lambda_{\min}\{\mathbf{y}_i^T \mathbf{y}_i\}$).

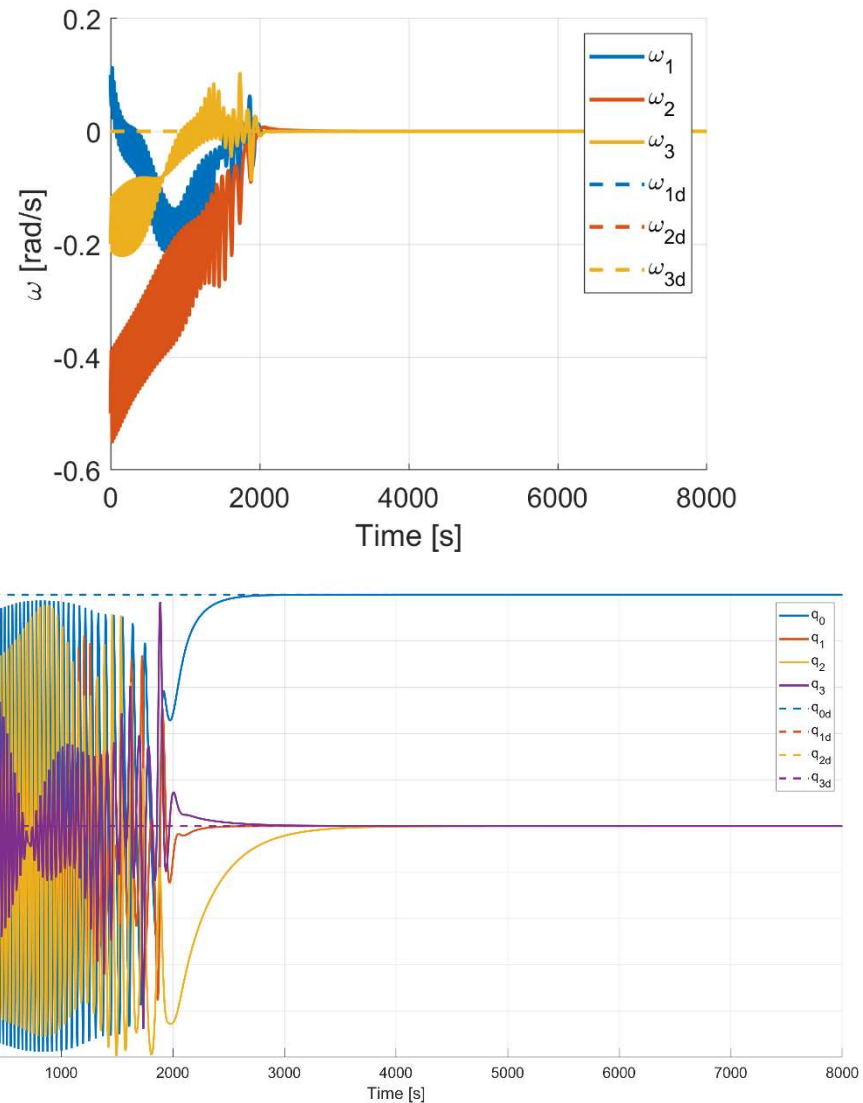


Figure 7 Sim 2 (ICL on) numerical results: spacecraft angular velocity vs desired angular velocity (top), spacecraft quaternion vs desired quaternion (bottom).

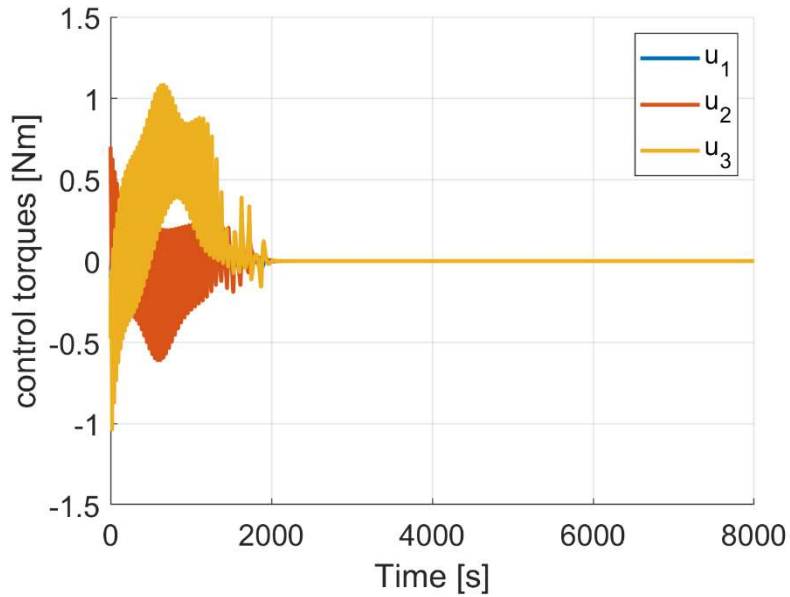


Figure 8 Sim 2 (ICL on) numerical results: spacecraft control torques.

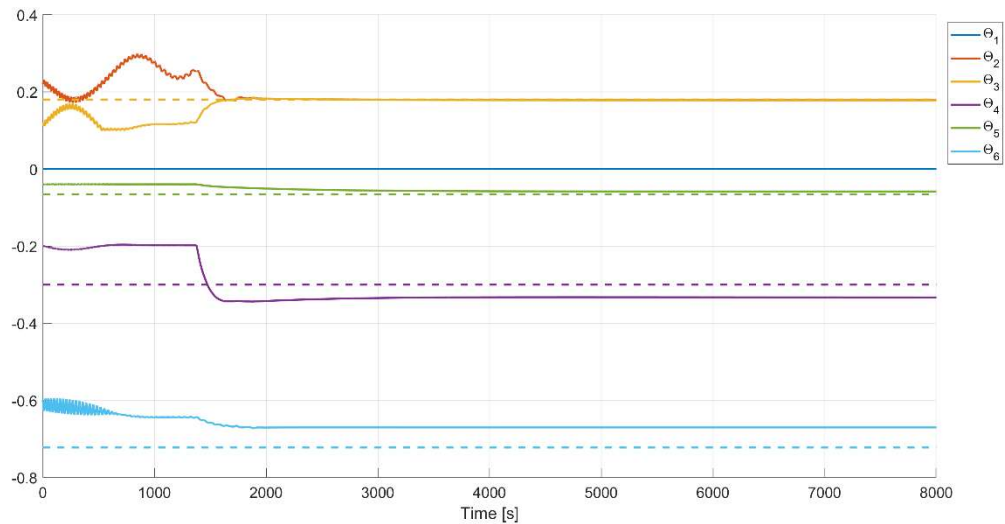


Figure 9 Sim 2 (ICL on) numerical results: vector of estimated unknowns vs true values.

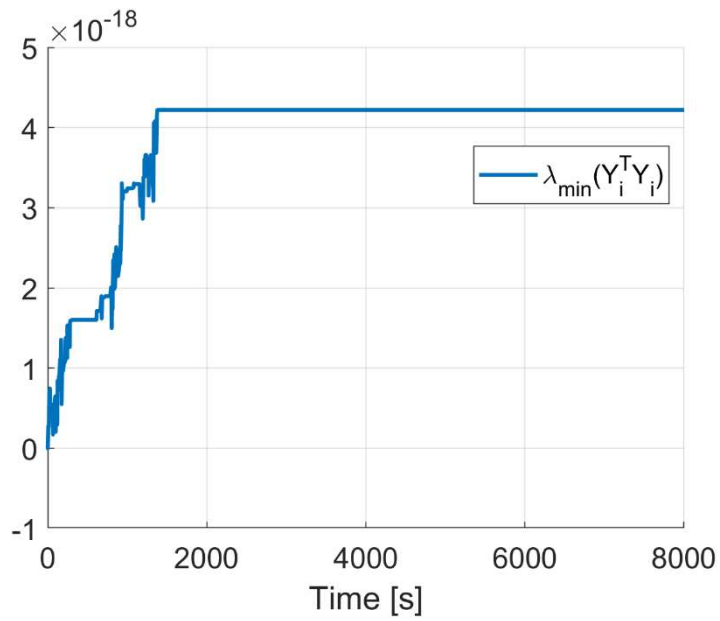


Figure 10 Sim 2 (ICL on) numerical results: finite excitation condition (eigenvalue in Equation 10).

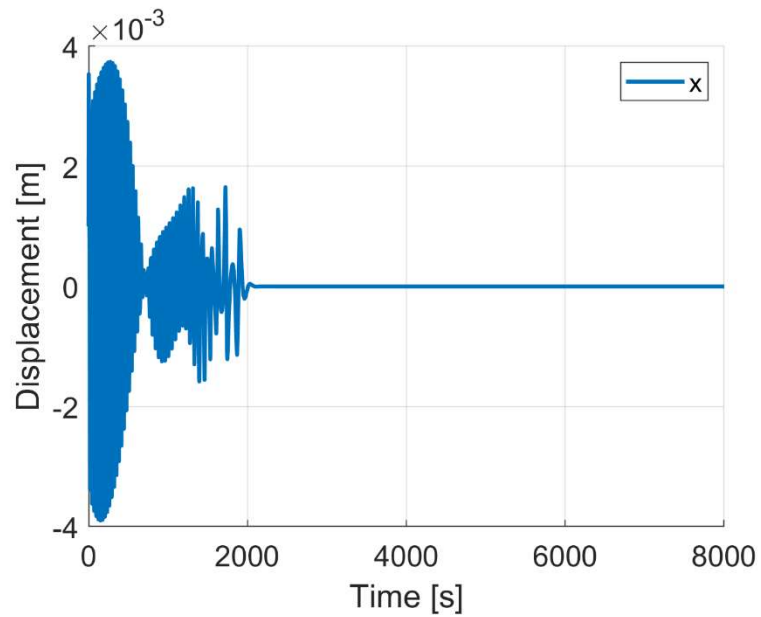


Figure 11 Sim 2 (ICL on) numerical results: lumped mass displacement.

The controller in Sim 2 required control gains that excited the system much more, as compared to the non-ICL counterpart. This requirement was noticed due to the small (almost non-existent) increase of the amplitude of $\lambda_{min}\{\mathbf{y}_i^T \mathbf{y}_i\}$ with gains similar to those used in Sim 1, indicating that the system might not be accumulating sufficient knowledge about the model during the transient, which could result in poor identification of the uncertain parameters. By manipulating the gains, the resulting controller has a significantly greater activity during the transient, moving the mass (m) so that its behavior is better captured by the ICL-based adaptation law. The uniformly ultimately bounded result can be clearly observed since the estimations converged to a vicinity of their real values, but despite this limitation, the a priori knowledge of Θ was clearly improved.

The final value of the vector of uncertain parameters for Sim 2 was $\widehat{\Theta} = [0, 0.178634, 0.177981, -0.333368, -0.0584866, -0.670413]^T$, using these values to recover ω_n and ζ we obtain

$$\omega_n = 1.4181 \text{ rad/s} , \quad \zeta = 0.0619$$

as opposed to the true values:

$$\omega_n = 1.0973 \text{ rad/s} , \quad \zeta = 0.05$$

The current results are promising and certainly need further investigation to improve the ultimately bounded result and reduce the estimation errors.

CONCLUSION

Adaptive control combined with integral concurrent learning holds the potential for simultaneous spacecraft attitude control and estimation of flexible parameters, while on-orbit. Application examples include input shaping for fast slewing maneuvers (e.g.: re-shaped bang-bang feedforwards), where a simple feedback or adaptive control would not be sufficient unless the natural frequencies and damping ratios are known. The next steps include generalization to dynamics models requiring a generic number of mass-spring-damper subsystems, located at different orientations and parts of the main spacecraft body. Another topic of future investigation should be limiting the amplitude for the excitation of the modes, currently not included in the Lyapunov formulation.

ACKNOWLEDGEMENTS

This work was initiated while Dr. Bevilacqua was an awardee of the 2021 Air Force Research Laboratory Summer Faculty Fellowship Program, working in collaboration with Dr. Sinclair.

REFERENCES

- ^{1.} L. D. Davis and A. J. Sinclair, “Demonstration science experiment adaptive control experiment plan & preliminary system identification” paper AAS 20-729. Astrodynamics Specialist Conference 2020.
- ^{2.} Romano, M., Agrawal, B.N., Bernelli Zazzera, F.: Experiments on Command Shaping Control of a Manipulator with Flexible Links. Journal of Guidance, Control, and Dynamics, Vol. 25, No. 2, 2002, pp. 232-239. (<http://dx.doi.org/10.2514/2.4903>).
- ^{3.} L.W. Taylor, On-Orbit Systems Identification of Flexible Spacecraft, IFAC Proceedings Volumes, Volume 18, Issue 5, 1985, Pages 511-516, ISSN 1474-6670, [https://doi.org/10.1016/S1474-6670\(17\)60611-6](https://doi.org/10.1016/S1474-6670(17)60611-6).
- ^{4.} Y. Xie et al., On-orbit identification of flexible parameters of spacecraft, Volume: 230 issue: 2, page(s): 191-206, 2016.

5. Camilo Riano-Rios, Riccardo Bevilacqua, Warren E. Dixon. 2020 Differential Drag-Based Multiple Spacecraft Maneuvering and On-Line Parameter Estimation Using Integral Concurrent Learning. Volume 174, September 2020, Pages 189-203, Acta Astronautica, <https://www.sciencedirect.com/science/article/pii/S0094576520302745>
6. Camilo Riano-Rios, Runhan Sun, Riccardo Bevilacqua, Warren E. Dixon, Aerodynamic and Gravity Gradient based Attitude Control for CubeSats in the presence of Environmental and Spacecraft Uncertainties, submitted to Acta Astronautica.
7. Runhan Sun, Camilo Riano-Rios, Riccardo Bevilacqua, Norman G. Fitz-Coy, and Warren E. Dixon, CubeSat Adaptive Attitude Control with Uncertain Drag Coefficient and Atmospheric Density, submitted to the Journal of Guidance, Control, and Dynamics.
8. <https://www.afrl.af.mil/News/Article/2402793/afrls-newest-lab-to-boost-nations-space-capabilities/> [retrieved April 6, 2021]
9. K. Bell, R. Moser, M. Powers, and S. Erwin, "A Deployable Optical Telescope Ground Demo", Proceedings of SPIE, 2000.
10. S.A. Lane, S.L. Lacy, V. Babuska , S. Hanes, K. Schrader, and R. Fuentes, "Active Vibration Control of a Deployable Optical Telescope", Journal of Spacecraft and Rockets, Vol. 45, No. 3, 2008, pp. 568 586.
11. <http://www.etegent.com/uploads/pdfs/project%20archives/MACE.pdf> [retrieved April 6, 2021]
12. <https://universitynanosat.org/> [retrieved March 7, 2021].
13. Sanny Omar, Camilo Riano-Rios, Riccardo Bevilacqua, "The Drag Maneuvering Device for the Semi-Passive Three-Axis Attitude Stabilization of Low Earth Orbit Nanosatellites', the Journal of Small Satellites (JoSS), Vol. 10, No. 01 (Feb. 2021), pp. 943–957.